IOP Conf. Series: Journal of Physics: Conf. Series **826** (2017) 012013 doi:10.1088/1742-6596/826/1/012013

Plasmon effects in photoemission

J. Z. Kamiński, F. Cajiao Vélez and K. Krajewska

Institute of Theoretical Physics, Faculty of Physics, University of Warsaw, Pasteura 5, 02-093 Warszawa, Poland

E-mail: Jerzy.Kaminski@fuw.edu.pl

Abstract. Recently, we observe an increasing interest in the laser-assisted processes that take place at the solids surfaces or at the interfaces of semiconductor heterostructures. These processes are affected by the plasmon effects induced by the interaction of quasi-free electrons in solids with laser fields. The plasmon effects lead to a significant enhancement of the oscillating in time electric field in a vicinity of the surface. The latter strongly modifies processes such as the high-order harmonic generation from atoms passing close to the surface, the electron photoemission from metal tips or the tunneling processes in semiconductor heterostructures. In our paper, we focus on the photoemission phenomenon accounting for the space-dependence of an oscillating in time, effective electric field created at the surface.

1. Introduction

The aim of this paper is to investigate the photoemission from a semiconductor heterostructure occurring in an arbitrary space-dependent scalar potential and a time- and space-dependent vector potential. The vector potential is periodic in time and describes a laser field. Its space-dependence results from the interaction of the laser field with electrons in solids. Such conditions are met, for example, in semiconductor nano-structures [1, 2, 3, 4, 5] (like quantum wires or wells), photoemission from a metal tip [6, 7], carbon nano-tubes or graphene [8, 9, 10] or in surface physics [11, 12, 13, 14, 15, 16, 17, 18, 19, 20]. To make our presentation as clear as possible we shall restrict ourselves to the one-space-dimensional case, although extension of the presented method to systems of higher dimensionality is possible (see, e.g. [21, 22]).

This paper is organized as follows. In Sec. II the most general solution of the Schrödinger equation is introduced. The transfer-matrix method and matching conditions are analyzed in Sec. III, whereas the reflection and transition probabilities are introduced in Sec. IV. These probabilities must sum up to 1, which puts a very strong check for the accuracy of our numerical calculations. The most important part of this paper, i.e., the concept of the scattering-matrix method, is discussed in Sec. V. It is shown there why the scattering-matrix algorithm has to be introduced, instead of a much simpler transfer-matrix algorithm. Numerical illustrations of the applicability of this algorithm are presented in Sec. VI and are followed by short conclusions.

Unless it is stated otherwise, atomic units are used in our numerical illustrations.

2. Solution of the Schrödinger equation

Let us start with the one-dimensional Schrödinger equation of the form [23],

$$\mathrm{i}\partial_t\psi(x,t) = \Big[\frac{1}{2}\Big(\frac{1}{\mathrm{i}}\partial_x - eA(x,t)\Big)\frac{1}{m(x)}\Big(\frac{1}{\mathrm{i}}\partial_x - eA(x,t)\Big) + V(x)\Big]\psi(x,t). \tag{1}$$

We assume that the space-dependent mass $m(x)$, scalar potential $V(x)$, and vector potential $A(x,t)$ are spatially constant in finite intervals. Their values in an interval (x_{i-1}, x_i) are denoted as m_i, V_i, and $A_i(t)$. We require also that the function $A(x,t)$ is periodic in time,

$$A(x, t+T) = A(x,t), \tag{2}$$

where $T = 2\pi/\omega$ and ω is the frequency of the oscillating in time electric field. Defining the probability density $\rho(x,t)$,

$$\rho(x,t) = |\psi(x,t)|^2, \tag{3}$$

and the probability current $j(x,t)$,

$$j(x,t) = \frac{1}{2}\psi^*(x,t)\frac{1}{m(x)}\Big(\frac{1}{\mathrm{i}}\partial_x - eA(x,t)\Big)\psi(x,t) + \frac{1}{2}\psi(x,t)\frac{1}{m(x)}\Big[\Big(\frac{1}{\mathrm{i}}\partial_x - eA(x,t)\Big)\psi(x,t)\Big]^*, \tag{4}$$

we show, using Eq. (1), that the probability is conserved. Indeed, assuming the above definitions, we obtain the continuity equation,

$$\partial_t \rho(x,t) + \partial_x j(x,t) = 0. \tag{5}$$

The space dependence of mass in Eq. (1) forces one to impose non-standard continuity conditions on any solution of this equation. It is now the wave-function $\psi(x,t)$ and the quantity

$$\frac{1}{m(x)}\Big(\frac{1}{\mathrm{i}}\partial_x - eA(x,t)\Big)\psi(x,t) \tag{6}$$

that have to be continuous at points of discontinuity of mass $m(x)$ and both potentials, $V(x)$ and $A(x,t)$ [23, 24, 25, 26]. We denote a general solution $\psi(x,t)$ of Eq. (1) in a given interval (x_{i-1}, x_i) as $\psi_i(x,t)$. Note that, due to time periodicity of the Hamiltonian, $\psi_i(x,t)$ can be chosen such that the Floquet condition,

$$\psi_i(x, t+T) = \mathrm{e}^{-\mathrm{i}ET}\psi_i(x,t), \tag{7}$$

is satisfied, where E is the so-called quasi-energy. In this case, $\psi_i(x,t)$ takes the form [28, 29, 30, 31],

$$\psi_i(x,t) = \sum_{M=-\infty}^{\infty} \exp\big(-\mathrm{i}(E+M\omega)t\big) \sum_{\sigma=\pm} \sum_{N=-\infty}^{\infty} C_{iN}^{\sigma} \mathcal{B}_{M-N}(\sigma p_{iN}) \exp\left(\mathrm{i}\sigma p_{iN} x\right), \tag{8}$$

where C_{iN}^{σ} are arbitrary complex numbers to be determined and

$$p_{iN} = \sqrt{2m_i(E + N\omega - V_i - U_i)}, \tag{9}$$

with $U_i = e^2\langle A_i^2(t)\rangle/2m_i$ being the ponderomotive energy. Here, $\langle A_i^2(t)\rangle$ means the time-average of $A_i^2(t)$ over the laser-field oscillations.

The components for which p_{iN} are purely imaginary are called the closed channels. These channels are not observed for a particle in initial or final states, but they have to be taken into account in order to satisfy the unitary condition of the time evolution. In a general case, $\mathcal{B}_{M-N}(\sigma p_{iN})$ is a component of the Fourier expansion,

$$\exp\big(\mathrm{i}\Phi_{iN}^{\sigma}(t)\big) = \sum_{M=-\infty}^{\infty} \exp\left(-\mathrm{i}M\omega t\right)\mathcal{B}_{M-N}(\sigma p_{iN}), \tag{10}$$

provided that the vector potential $A(x,t)$ is periodic in time. Functions $\Phi_{iN}^{\sigma}(t)$ are defined as follows:

$$\Phi_{iN}^{\sigma}(t) = \int_0^t \Big[\frac{\sigma e}{m_i} A_i(t) p_{iN} - \frac{e^2}{2m_i}\big(A_i^2(t) - \langle A_i^2(t)\rangle\big)\Big]\mathrm{d}t. \tag{11}$$

One can understand from these equations that the $\mathcal{B}_{M-N}(\sigma p_{iN})$ functions depend on the form of the vector potential $A(x,t)$ describing the laser field.

3. Matching conditions and transfer matrix

Continuity conditions discussed above and applied to a general solution (8) of the Schrödinger equation (1) lead to an infinite chain of equations connecting constants C^{σ}_{iN} in the neighboring domains. These matching conditions can be written in the matrix form,

$$B(i-1,x_{i-1})C_{i-1} = B(i,x_{i-1})C_i, \tag{12}$$

where $C^{\pm}_{iN} = [C^{\pm}_i]_N$ are the components of the columns $C^{\pm}_i$. The matrices $B(i,x)$ and C_i are defined as follows,

$$B(i,x) = \begin{pmatrix} B^+(i,x) & B^-(i,x) \\ B'^+(i,x) & B'^-(i,x) \end{pmatrix}, \; C_i = \begin{pmatrix} C^+_i \\ C^-_i \end{pmatrix}. \tag{13}$$

The elements of $B(i,x)$ can be computed in the following way.

For an arbitrary function $A(x,t)$ which satisfies Eq. (2), we have that

$$A(x,t) = \sum_{n=-\infty}^{\infty} b_n(x) \exp\left(-\mathrm{i}n\omega t\right). \tag{14}$$

The coefficients $b_n(x)$ assume constant values in the interval (x_{i-1}, x_i), which we shall denote as $b_{i,n}$. Using the continuity condition for the wave-function $\psi_i(x,t)$ at the point x_{i-1}, we compute the elements of the matrices B^+ and B^-,

$$B^{\pm}(i,x)_{M,N} = \mathcal{B}_{M-N}(\pm p_{i,N})\mathrm{e}^{\pm \mathrm{i}p_{i,N}x}. \tag{15}$$

On the other hand, elements of the B' matrix can be evaluated by substituting a general solution (8) to the expression (6) and applying the continuity condition at x_{i-1}. After some algebraic manipulations we finally obtain the expression for the B'-matrices,

$$B'^{\pm}(i,x)_{M,N} = \pm\frac{1}{m_i}\mathcal{B}_{M-N}(\pm p_{i,N})p_{i,N}\mathrm{e}^{\pm \mathrm{i}p_{i,N}x} - \frac{1}{m_i}\sum_{n=-\infty}^{\infty} eb_{i,n}\mathcal{B}_{M-N-n}(\pm p_{i,N})\mathrm{e}^{\pm \mathrm{i}p_{i,N}x}, \tag{16}$$

and a set of equations for vectors C_i,

$$C_i = B_i C_{i-1}, \tag{17}$$

where

$$B_i = [B(i,x_{i-1})]^{-1}B(i-1,x_{i-1}). \tag{18}$$

These relations allow to connect a solution in a given domain $x_{i-1} < x < x_i$ with an analogous solution in any other domain $x_{j-1} < x < x_j$,

$$C_j = B_j B_{j-1}, \ldots, B_{i+1}C_i = \mathcal{T}_{ji}C_i, \tag{19}$$

where $\mathcal{T}_{ji}$ is the so-called transfer matrix [27, 28, 25].

4. Reflection and transition probabilities

It is clear now that, on the basis of Eq. (19), we can connect solutions in the boundary domains $(-\infty, x_0)$ and (x_{L-1}, ∞). Values of mass $m(x)$, scalar potential $V(x)$ and vector potential $A(x,t)$ in these domains will be denoted as m_0, V_0, $A_0(t)$ and m_L, V_L, $A_L(t)$, respectively. We can then

write down solutions of (1) for each of these domains. These solutions represent incident ($\psi_{\rm inc}$), reflected ($\psi_{\rm ref}$), and transmitted ($\psi_{\rm tr}$) waves,

$$\psi_{\rm inc}(x,t) = \sum_{M=-\infty}^{\infty} {\rm e}^{-{\rm i}Et}{\rm e}^{-{\rm i}M\omega t}\mathcal{B}_M(p_0){\rm e}^{{\rm i}p_0 x}, \tag{20}$$

$$\psi_{\rm ref}(x,t) = \sum_{N,M=-\infty}^{\infty} C^-_{0,N}{\rm e}^{-{\rm i}Et}{\rm e}^{-{\rm i}M\omega t}\mathcal{B}_{M-N}(-p_N){\rm e}^{-{\rm i}p_N x}, \tag{21}$$

$$\psi_{\rm tr}(x,t) = \sum_{N,M=-\infty}^{\infty} C^+_{L,N}{\rm e}^{-{\rm i}Et}{\rm e}^{-{\rm i}M\omega t}\mathcal{B}_{M-N}(q_N){\rm e}^{{\rm i}q_N x}, \tag{22}$$

where

$$p_N = \sqrt{2m_0(E+N\omega-V_0-U_0)}, \quad q_N = \sqrt{2m_L(E+N\omega-V_L-U_L)}. \tag{23}$$

Constants $C^-_{0,N}$ and $C^+_{L,N}$ will be denoted from now on as ${\rm R}_N$ and ${\rm T}_N$, respectively. Using continuity conditions for the functions defined above, we get the probability conservation equation for reflection and transition amplitudes, ${\rm R}_N$ and ${\rm T}_N$,

$$\sum_{N\geqslant N_{\rm ref}} \frac{p_N}{p_0}|{\rm R}_N|^2 + \sum_{N\geqslant N_{\rm tr}} \frac{m_0 q_N}{m_L p_0}|{\rm T}_N|^2 = 1, \tag{24}$$

where summations are over such N for which p_N and q_N are real, i.e., over the open channels. This equation permits us to interpret

$$P_{\rm R}(N) = \frac{p_N}{p_0}|{\rm R}_N|^2 \tag{25}$$

and

$$P_{\rm T}(N) = \frac{m_0 q_N}{m_L p_0}|{\rm T}_N|^2 \tag{26}$$

as reflection and transition probabilities for a tunneling process in which absorption ($N>0$) or emission ($N<0$) of energy $N\omega$ by electrons occurred [28, 26]. In the case of a monochromatic laser field, this process can be interpreted as absorption or emission of N photons from the laser field.

The unitary condition (24) can be also interpreted as the conservation of the electric charge. If we define the quantities proportional to the density of electric currents,

$$J_{\rm inc} = \frac{p_0}{m_0}, \quad J_{\rm ref} = \sum_{N\geqslant N_{\rm ref}} \frac{p_N}{m_0}|{\rm R}_N|^2, \quad J_{\rm tr} = \sum_{N\geqslant N_{\rm tr}} \frac{q_N}{m_L}|{\rm T}_N|^2, \tag{27}$$

then Eq. (24) has the form of the first Kirchhoff law,

$$J_{\rm inc} = J_{\rm ref} + J_{\rm tr}. \tag{28}$$

Using Eq. (19) we can calculate constants $C^-_{0,N} = {\rm R}_N$ and $C^+_{L,N} = {\rm T}_N$ appearing in equations (20) - (22). Indeed, since

$$C_L = \mathcal{T} C_0, \tag{29}$$

where the transfer matrix $\mathcal{T} = \mathcal{T}_{L0}$, and because $\mathcal{T}$, C_0, and C_L have the following block forms,

$$\mathcal{T} = \begin{pmatrix} \mathcal{T}^{++} & \mathcal{T}^{+-} \\ \mathcal{T}^{-+} & \mathcal{T}^{--} \end{pmatrix}, \quad C_0 = \begin{pmatrix} C_0^+ \\ {\rm R} \end{pmatrix}, \quad C_L = \begin{pmatrix} {\rm T} \\ 0 \end{pmatrix}, \tag{30}$$

we arrive at

$$\mathrm{T} = \mathcal{T}^{++}C_0^+ + \mathcal{T}^{+-}\mathrm{R}, \quad 0 = \mathcal{T}^{-+}C_0^+ + \mathcal{T}^{--}\mathrm{R}. \tag{31}$$

Here, R and T denote the columns of R_N and T_N, and $[C_0^+]_N = \delta_{0,N}$. Thus, after some algebraic manipulations, we obtain

$$\mathrm{R} = -(\mathcal{T}^{--})^{-1}\mathcal{T}^{-+}C_0^+, \quad \mathrm{T} = \big(\mathcal{T}^{++} - \mathcal{T}^{+-}(\mathcal{T}^{--})^{-1}\mathcal{T}^{-+}\big)C_0^+, \tag{32}$$

which allows us to determine the quantities R_N and T_N for a given transfer matrix $\mathcal{T}$. For open channels, these quantities are the amplitudes of reflection (R_N) and transition (T_N) probabilities, from which one can compute reflection and transition probabilities using equations (25) and (26).

5. The scattering matrix

It follows from equations (15) and (16) that each of the B_i matrices that constitute the transfer matrix $\mathcal{T}_{ji}$ contain elements $\exp(\pm \mathrm{i}p_{i,N}x_i)$. The latter depend on the x_i coordinates at which the discontinuities appear. For closed channels, that is when the $p_{i,N}$ momenta are purely imaginary, these numbers are real and may assume arbitrary values, depending on the x_i coordinates. The number of B_i matrices is equal to the number of discontinuity points, i.e., it depends on how we divide the space into short intervals in order to make our potential tractable by our algorithm. It may, therefore, turn out that in order to compute the transfer matrix $\mathcal{T}_{ji}$, we have to multiply a large number of the B_i matrices, each containing both very small and very large numbers. It is clear that such a procedure is numerically unstable. We have to find a way to modify our method of calculations in order to compute the elements of each B_i matrix at the same point $x = 0$ independently of where the 'real' x_i is. This would eliminate "dangerous" $\exp(\pm \mathrm{i}p_{i,N}x_i)$ elements (turning them to 1), however at the cost of appearing somewhere else. We shall see later that these 'left-overs' appear only as differences $x_{i+1} - x_i$ and, therefore, do not cause any harmful side-effects.

It follows from Eq. (19) that in the neighboring domains, (x_{i-2}, x_{i-1}) and (x_{i-1}, x_i), we have,

$$C_i = \mathcal{T}_{i,i-1}C_{i-1}. \tag{33}$$

Although the elements of the transfer matrix $\mathcal{T}_{i,i-1}$ have been computed from the continuity conditions at point x_{i-1}, one can compute them at any other point, for example at $x = 0$. To this end, let us note what follows from the solution (8). Translation of the system by a certain distance δ along the x-axis causes only multiplication of each member of the sum over N in (8) by a constant $\exp(\mathrm{i}\sigma p_{iN}\delta)$. These constants can be included into the coefficients C_{iN}^σ. In this way, we obtain a new set of constants which we shall denote as $\tilde{C}_{iN}^\sigma$,

$$\tilde{C}_{iN}^\sigma = \exp(\mathrm{i}\sigma p_{iN}\delta)C_{iN}^\sigma. \tag{34}$$

We shall interpret these constants as coefficients in the solution (8), given by the continuity conditions at a point $x_{i-1} - \delta$. Eq. (34), written in the matrix form, becomes

$$\tilde{C}_i = \mathcal{P}_i(\delta)C_i, \tag{35}$$

where

$$\mathcal{P}_i(\delta) = \begin{pmatrix} P_i^+(\delta) & 0 \\ 0 & P_i^-(\delta) \end{pmatrix} \tag{36}$$

and

$$C_i = \begin{pmatrix} C_i^+ \\ C_i^- \end{pmatrix}, \tilde{C}_i = \begin{pmatrix} \tilde{C}_i^+ \\ \tilde{C}_i^- \end{pmatrix}. \tag{37}$$

In the equation above, $P_i^{\sigma}(\delta)$ is a diagonal matrix,

$$[P_i^{\sigma}(\delta)]_{NN'} = \delta_{NN'} \exp\left(\mathrm{i}\sigma p_{iN}\delta\right), \tag{38}$$

whereas $C_i^{\pm}$ and $\tilde{C}_i^{\pm}$ are the columns consisting of the constants $C_{iN}^{\pm}$ and $\tilde{C}_{iN}^{\pm}$, respectively, that is $[C_i^{\pm}]_N = C_{iN}^{\pm}$ and $[\tilde{C}_i^{\pm}]_N = C_{iN}^{\pm}$. It follows from the form of the matrix $\mathcal{P}_i(\delta)$ that the following relations are satisfied,

$$\mathcal{P}_i^{-1}(\delta) = \mathcal{P}_i(-\delta), \quad \mathcal{P}_i(\delta_1)\mathcal{P}_i(\delta_2) = \mathcal{P}_i(\delta_1+\delta_2). \tag{39}$$

Let us also note that the translation of the system defined above modifies the transfer matrix $\mathcal{T}_{i,i-1}$. We have

$$\mathcal{P}_i^{-1}\tilde{C}_i = C_i = \mathcal{T}_{i,i-1}C_{i-1} = \mathcal{T}_{i,i-1}\mathcal{P}_{i-1}^{-1}(\delta)\mathcal{P}_{i-1}(\delta)C_{i-1}. \tag{40}$$

Thus,

$$\tilde{C}_i = \mathcal{P}_i(\delta)\mathcal{T}_{i,i-1}\mathcal{P}_{i-1}^{-1}(\delta)\tilde{C}_{i-1} \tag{41}$$

and we can write it down as

$$\tilde{C}_i = \tilde{\mathcal{T}}_{i,i-1}\tilde{C}_{i-1}, \tag{42}$$

where

$$\tilde{\mathcal{T}}_{i,i-1} = \mathcal{P}_i(\delta)\mathcal{T}_{i,i-1}\mathcal{P}_{i-1}^{-1}(\delta). \tag{43}$$

Matrix elements denoted with the tilde symbol refer to the translated system. Using the method defined above and the relation (19), we can connect now the solution in the domain $(-\infty, x_0)$ with the solution in any other domain (x_{i-1}, x_i). In this way the elements of the transfer matrix, which until now have been computed at the points of discontinuity $x_0 \dots x_{i-1}$, are computed each time at the same point $x = 0$. Let us illustrate this method for a special case of $i = 3$

$$\begin{aligned} C_3 &= \mathcal{T}_{3,2}\mathcal{T}_{2,1}\mathcal{T}_{1,0}C_0 = \mathcal{P}_3^{-1}(x_2)\mathcal{T}_{3,2}^0\mathcal{P}_2(x_2)\mathcal{P}_2^{-1}(x_1)\mathcal{T}_{2,1}^0\mathcal{P}_1(x_1)\mathcal{P}_1^{-1}(x_0)\mathcal{T}_{1,0}^0\mathcal{P}_0(x_0)C_0 \\ &= \mathcal{P}_3^{-1}(x_2)\mathcal{T}_{3,2}^0\mathcal{P}_2(x_2-x_1)\mathcal{T}_{2,1}^0\mathcal{P}_1(x_1-x_0)\mathcal{T}_{1,0}^0\mathcal{P}_0(x_0)C_0. \end{aligned} \tag{44}$$

Eq. (44) connects constants C_0 and C_3 using the matrices $\mathcal{T}_{j,j-1}^0$ calculated at $x = 0$ independently of j, and the diagonal matrices $\mathcal{P}_j(\delta_j)$, given by the relations (36) and (38), where $\delta_j = x_j - x_{j-1}$. The edge matrices $\mathcal{P}_0(x_0)$ and $\mathcal{P}_3^{-1}(x_2)$ in Eq. (44) can be omitted while computing the transmission and reflection probability amplitudes, as their only role is to multiply the amplitudes by phase quotients which disappear while computing the probabilities. Although these matrices lead to significant modifications of the closed channels in the domains of $x < x_0$ and $x > x_3$, these channels do not influence the reflection and transition amplitudes. Transmission and reflection probabilities can thus be computed using a modified transfer matrix,

$$\mathcal{T}_{3,0}^0 = \mathcal{T}_{3,2}^0\mathcal{P}_2(x_2-x_1)\mathcal{T}_{2,1}^0\mathcal{P}_1(x_1-x_0)\mathcal{T}_{1,0}^0. \tag{45}$$

The matrices $\mathcal{T}_{i,i-1}^0$ are equal to the matrices B_i in Eq. (18) calculated, however, for $x_{i-1} = 0$. This speeds up numerical calculations since now the matrix $B(i, x = 0)$ in Eq. (18) have to be inverted only once. Further, we shall omit the superscript 0 in $\mathcal{T}$ and the tilde over C in order to simplify our notation.

The method presented above is still numerically unstable. The reason for this instability is the existence of large numerical values of elements of $\mathcal{P}_i^{-}(\delta)$ for imaginary momenta p_{iN}. In other words, for

$$C_i = \begin{pmatrix} C_i^+ \\ C_i^- \end{pmatrix} = \mathcal{T}_{i,i-1}C_{i-1} = \begin{pmatrix} \mathcal{T}_{i,i-1}^{++} & \mathcal{T}_{i,i-1}^{+-} \\ \mathcal{T}_{i,i-1}^{-+} & \mathcal{T}_{i,i-1}^{--} \end{pmatrix} \begin{pmatrix} C_{i-1}^+ \\ C_{i-1}^- \end{pmatrix}, \tag{46}$$

the source of numerical instabilities are matrix elements $\mathcal{T}^{--}_{i,i-1}$ that contain large numbers. There is, however, a chance for improving the stability, if only its inverse will be used, $\left(\mathcal{T}^{--}_{i,i-1}\right)^{-1}$. This is possible provided that in our numerical algorithm only the so-called scattering matrix will be applied. For this reason we will show below how to compute the scattering matrix, $\mathcal{S}_{j,i}$, using only elements of the transfer matrix, $\mathcal{T}_{j,i}$. For the transfer matrix $\mathcal{T}_{j,i}$ we have,

$$\begin{pmatrix} C^+_j \\ C^-_j \end{pmatrix} = \begin{pmatrix} \mathcal{T}^{++}_{j,i} & \mathcal{T}^{+-}_{j,i} \\ \mathcal{T}^{-+}_{j,i} & \mathcal{T}^{--}_{j,i} \end{pmatrix} \begin{pmatrix} C^+_i \\ C^-_i \end{pmatrix}. \tag{47}$$

Thus,

$$C^+_j = \mathcal{T}^{++}_{j,i} C^+_i + \mathcal{T}^{+-}_{j,i} C^-_i, \quad C^-_j = \mathcal{T}^{-+}_{j,i} C^+_i + \mathcal{T}^{--}_{j,i} C^-_i. \tag{48}$$

On the basis of (48) we now want to compute the elements of the $\mathcal{S}_{j,i}$ matrix. This matrix is supposed to connect the coefficients $C^\pm_i$ and $C^\pm_j$ in the following way,

$$\begin{pmatrix} C^-_i \\ C^+_j \end{pmatrix} = \begin{pmatrix} \mathcal{S}^{++}_{j,i} & \mathcal{S}^{+-}_{j,i} \\ \mathcal{S}^{-+}_{j,i} & \mathcal{S}^{--}_{j,i} \end{pmatrix} \begin{pmatrix} C^+_i \\ C^-_j \end{pmatrix}. \tag{49}$$

Using the set of linear equations (48), we easily compute the coefficients C^-_i and C^+_j on the left-hand side of equation (49) as functions of the coefficients C^-_j and C^+_i. We obtain then the following relations,

$$\begin{aligned} C^-_i &= (\mathcal{T}^{--}_{j,i})^{-1}(C^-_j - \mathcal{T}^{-+}_{j,i} C^+_i), \\ C^+_j &= \left(\mathcal{T}^{++}_{j,i} - \mathcal{T}^{+-}_{j,i}(\mathcal{T}^{--}_{j,i})^{-1}\mathcal{T}^{-+}_{j,i}\right) C^+_i + \mathcal{T}^{+-}_{j,i}(\mathcal{T}^{--}_{j,i})^{-1} C^-_j. \end{aligned} \tag{50}$$

Finally, we compute the elements of the matrix $\mathcal{S}_{j,i}$,

$$\begin{aligned} \mathcal{S}^{++}_{j,i} &= -(\mathcal{T}^{--}_{j,i})^{-1}\mathcal{T}^{-+}_{j,i}, & \mathcal{S}^{+-}_{j,i} &= (\mathcal{T}^{--}_{j,i})^{-1}, \\ \mathcal{S}^{-+}_{j,i} &= \mathcal{T}^{++}_{j,i} - \mathcal{T}^{+-}_{j,i}(\mathcal{T}^{--}_{j,i})^{-1}\mathcal{T}^{-+}_{j,i}, & \mathcal{S}^{--}_{j,i} &= \mathcal{T}^{+-}_{j,i}(\mathcal{T}^{--}_{j,i})^{-1}. \end{aligned} \tag{51}$$

As expected, the matrix $\mathcal{S}_{j,i}$ contains only numerically stable elements $(\mathcal{T}^{--}_{j,i})^{-1}$.

It follows from Eq. (19) that the transfer matrix $\mathcal{T}_{j,i}$ can be written as the product of two transfer matrices, $\mathcal{T}_{j,k}$ and $\mathcal{T}_{k,i}$ $(i < k < j)$,

$$\mathcal{T}_{j,i} = \mathcal{T}_{j,k}\mathcal{T}_{k,i}, \tag{52}$$

where matrices $\mathcal{T}_{j,k}$ and $\mathcal{T}_{k,i}$ are defined as follows,

$$C_k = \mathcal{T}_{k,i} C_i, \quad C_j = \mathcal{T}_{j,k} C_k. \tag{53}$$

Applying the method presented above, for each of the transfer matrices $\mathcal{T}_{j,k}$ and $\mathcal{T}_{k,i}$ we can now construct a scattering matrix, $\mathcal{S}_{j,k}$ and $\mathcal{S}_{k,i}$, respectively. The elements of the scattering matrix $\mathcal{S}_{j,i}$ can be computed using only elements of $\mathcal{S}_{j,k}$ and $\mathcal{S}_{k,i}$. Using the notation above, we obtain the following expressions for the elements of the $\mathcal{S}_{j,i}$ matrix,

$$\begin{aligned} \mathcal{S}^{++}_{j,i} &= \mathcal{S}^{++}_{k,i} + \mathcal{S}^{+-}_{k,i}(1 - \mathcal{S}^{++}_{j,k}\mathcal{S}^{--}_{k,i})^{-1}\mathcal{S}^{++}_{j,k}\mathcal{S}^{-+}_{k,i}, \quad \mathcal{S}^{+-}_{j,i} = \mathcal{S}^{+-}_{k,i}(1 - \mathcal{S}^{++}_{j,k}\mathcal{S}^{--}_{k,i})^{-1}\mathcal{S}^{+-}_{j,k}, \\ \mathcal{S}^{--}_{j,i} &= \mathcal{S}^{--}_{j,k} + \mathcal{S}^{-+}_{j,k}\mathcal{S}^{--}_{k,i}(1 - \mathcal{S}^{++}_{j,k}\mathcal{S}^{--}_{k,i})^{-1}\mathcal{S}^{+-}_{j,k}, \quad \mathcal{S}^{-+}_{j,i} = \mathcal{S}^{-+}_{j,k}(1 - \mathcal{S}^{++}_{j,k}\mathcal{S}^{--}_{k,i})^{-1}\mathcal{S}^{-+}_{k,i}. \end{aligned} \tag{54}$$

It is clear that the $\mathcal{S}_{j,i}$ matrix is not merely a product of two matrices $\mathcal{S}_{j,k}$ and $\mathcal{S}_{k,i}$, but rather a complicated nonlinear composition of them. It is important, however, to note that, despite its complexity, such a construction of the scattering matrix is numerically stable. This is in contrast to the transfer matrix method which fails if a system with a large number of discontinuity points x_i is considered. Stability of such an algorithm has been proven in our numerical investigations by checking that the condition (24) is satisfied with an error smaller than 10^{-14}. Such an accuracy can never be achieved for systems with a large number of discontinuity points if the transfer matrix is applied.

6. Photoemission

In our studies, we focus on essential features of the solid-vacuum interface, as demonstrated by the Sommerfeld model in which the band structure is neglected. This simplification allows us to consider a quite general form of the laser field. To be more specific, the solid surface is described by a continuous step potential,

$$V(x) = V_0 g(x/w_0), \quad g(x) = 1/(1+\mathrm{e}^{-x}). \tag{55}$$

The parameter w_0 determines the skin depth of a surface. For $w_0 = 0$, the surface potential represents the step function, commonly used in the Sommerfeld model. In our illustrations, we take $w_0 = 5$. We apply our theory to the gold surface and assume that the electron effective mass is close to the free electron mass. The work function and the Fermi energy for the gold metal are equal to 5.1 eV and 5.53 eV, respectively. This means that the constant V_0 above (as the sum of the work function and the Fermi energy) equals 10.63 eV.

The surface potential described above can be generalized further to meet conditions suitable for other solids. In particular, one can take into account the space-dependent effective mass of electrons in semiconductor heterostructures or metals with effective masses different from the free electron mass.

On the other hand, the form of the laser field is assumed to depend on both space and time coordinates. Since, for laser pulses of duration $\sim$ 30 fs and 800 nm wavelength, the monochromatic approximation works well, we use the following form of the laser electric field:

$$\mathcal{E}(x,t) = \mathcal{E}_0(x)\sin(\omega t) = \mathcal{E}_0 f_L(x)\big(1+\epsilon f_P(x)\big)\sin(\omega t), \tag{56}$$

where

$$f_L(x) = g(x/\zeta_L - a_L)g(b_L - x/\mu_L), \quad f_P(x) = g(x/\zeta_P - a_P)g(b_P - x/\mu_P). \tag{57}$$

The parameter ϵ defines the plasmon-enhanced part of the laser field. We choose the Ti:sapphire laser beam of frequency $\omega = 1.5498$ eV ($\lambda = 800$ nm). This means that, inside the solid, the laser field intensity averaged over the time period decays exponentially, $I(x) \sim \mathrm{e}^{2x/\zeta_L}$. On the other hand, in vacuum, it stays constant close to the surface, and then again decays exponentially. In this way, we can mimic a real physical situation in which the radiation-filled space is finite. In our illustrations, we take $\zeta_L = 40$, which means that the penetration depth of the laser field equals $\zeta_L/2 = 20$. The parameter $a_L\zeta_L$ describes the distance in a solid at which the intensity is not reduced substantially. On the other hand, $b_L\mu_L$ corresponds to the laser focus diameter in vacuum, whereas μ_L alone determines the intensity reduction rate outside the focus. Similar parameters with the subscript P refer to the plasmon-enhanced part of the laser field. The remaining parameters have been chosen as follows: $a_L = 3$, $b_L = 20$, $\mu_L = 100$, $a_P = 1$, $\zeta_P = 8$, $b_P = 4$, $\mu_P = 20$, and $\epsilon = 0, \ldots, 5$. All dimensional parameters are in atomic units.

In our discussion below, the laser field intensity is characterized by the dimensionless parameter $\xi = U_p/\omega$, where $U_p = \mathcal{E}_0^2/(4\omega^2)$ is the ponderomotive energy of electrons in the monochromatic plane wave of frequency ω; hence $\mathcal{E}_0 = 2\omega\sqrt{\omega\xi}$. In Fig. 1 we draw the space-dependence of the continuous step potential $V(x)$ and the electric field amplitude $\mathcal{E}_0(x)$ for $\epsilon = 5$ and $\xi = 0.1$.

The total photoemission probability is equal to

$$P_{\mathrm{T}} = \sum_{N \geqslant N_{\mathrm{tr}}} \frac{m_0 q_N}{m_L p_0} |\mathrm{T}_N|^2. \tag{58}$$

We plot it in Fig. 1 as a function of the electron kinetic energy for $\xi = 0.1$ and for six values of ϵ. We clearly see the multi-photon structure in this distribution, i.e., the total probability jumps

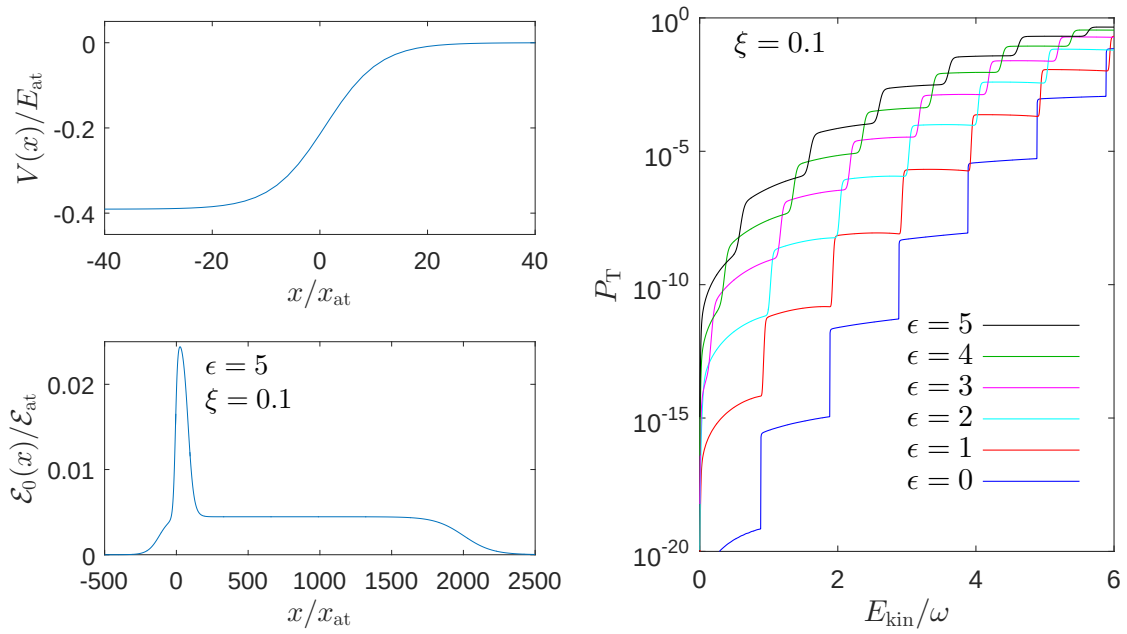

Figure 1. The continuous step potential (upper panel on the left) and the space-dependent electric field amplitude of the laser field (lower panel on the left). The atomic units of length, energy, and electric field strength are $x_{\rm at} \approx 0.053\,{\rm nm}$, $E_{\rm at} \approx 27.21{\rm eV}$, and $\mathcal{E}_{\rm at} \approx 5.14\times10^{11}\,{\rm V/m}$, respectively. In the right panel, we show total photoemission probabilities as functions of the kinetic energy of electrons for $\xi = 0.1$ and for six values of ϵ.

by few orders of magnitude if a smaller number of laser photons is sufficient for photoemission. As expected, the plasmon effect usually increases the photoemission probability. Moreover, the energy of the multi-photon channel opening increases with increasing ϵ, which is due to the increase of the space-dependent ponderomotive energy of the laser field. The significance of this effect for the tunneling phenomena is going to be discussed in due course.

7. Conclusions

As mentioned above, our numerical algorithm is convergent provided that a sufficient number of discrete points is introduced. For systems considered here, this number should not be smaller than 100. If the laser field is very weak, this does not create significant numerical problems, except that calculations become longer. However, when the laser field is sufficiently intense, the algorithm based on the transfer matrix is unstable. This instability is due to the existence of closed channels, which introduce into numerical calculations very small and very large numbers at the same time. The augmenting precision significantly slows down the calculation and does not diminish the problem. We have found that it is possible to make this algorithm numerically stable by applying non-linear matrix transformations, without introducing higher precisions.

Illustrations presented in this paper show that photoemission of electrons can be changed significantly by applying nonperturbative, oscillating in time and space-dependent electric fields. The efficiency of the numerical algorithm opens up the possibility of investigating surface phenomena in the presence of more realistic laser pulses that gradually decrease within solids and extend on a mesoscopic scale in vacuum.

Acknowledgements

We would like to thank Dr S. Varró for stimulating discussions during the LPHYS'16 conference.

References

[1] Hamilton K E, Kovalev A A, De A and Pryadko L P 2015 *J. Appl. Phys.* **117** 213103
[2] Faisal F H M and Genieser R 1989 *Phys. Lett. A* **141** 297
[3] Kamiński J Z 1993 *Acta Phys. Pol. A* **83** 495
[4] Klinovaja J, Stano P and Loss D 2016 *Phys. Rev. Lett.* **116** 176401
[5] Puviani M and Manghi F 2016 *Phys. Rev. B* **94** 161111(R)
[6] Kim S, Jin J, Kim Y-J, Park I-Y, Kim Y and Kim S-W 2008 *Nature* **453** 757
[7] Krüger M, Schenk M and Hommelhoff P 2011 *Nature* **475** 78
[8] Zhou Y and Wu M W 2011 *Phys. Rev. B* **83** 245436
[9] Khosravi H, Daneshfar N and Bahari A 2009 *Optics Lett.* **34** 1723
[10] Hsu H and Reichl L E 2006 *Phys. Rev. B* **74** 115406
[11] Mahmood F, Chan C-K, Alpichshev Z, Gardner D, Lee Y, Lee P A and Gedik N 2016 *Nat. Phys.* **12** 306
[12] Wang Y H, Steinberg H, Jarillo-Herrero P and Gedik N 2013 *Science* **342** 453
[13] Wang Z-B, Jiang H, Liu H and Xie X C 2015 *Solid State Commun.* **215-216** 18
[14] Faraggi M, Aldazabal I, Gravielle M S, Arnau A and Silkin V M 2009 *J. Opt. Soc. Am. B* **26** 2331
[15] Saathoff G, Miaja-Avila L, Aeschlimann M, Murnane M M and Kapteyn H C 2008 *Phys. Rev. A* **77** 022903
[16] Faraggi M N, Gravielle M S and Mitnik D M 2007 *Phys. Rev. A* **76** 012903
[17] Dombi P, Krausz F and Farkas G 2006 *J. Mod. Opt.* **53** 163
[18] Varró S and Kroó N 2011 *Appl. Phys. B* **105** 509
[19] Kroó N, Rácz and Varró S 2015 *EPL* **110** 67008
[20] Kroó N, Varró S, Rácz and Dombi P 2016 *Phys. Scr.* **91** 053010
[21] Faisal F H M, Kamiński J Z and Saczuk E 2005 *Phys. Rev. A* **72** 023412
[22] Faisal F H M, Kamiński J Z and Saczuk E 2006 *Laser Phys.* **16** 272
[23] Lévy-Leblond J-M 1992 *Eur. J. Phys.* **13** 215
[24] Kamiński J Z and Ehlotzky F 1999 *J. Phys. B* **32** 3193
[25] Moiseyev N and Lefebvre R 2001 *Phys. Rev. A* **64** 052711
[26] Saczuk E and Kamiński J Z 2003 *Phys. Stat. Sol. (b)* **240** 603
[27] Tsu R and Esaki L 1973 *Appl. Phys. Lett.* **22** 562
[28] Kamiński J Z 1990 *Z. Phys. D* **16** 153
[29] Faisal F H M and Kamiński J Z 1997 *Phys. Rev. A* **56** 748
[30] Faisal F H M and Kamiński J Z 1996 *Phys. Rev. A* **54**, R1769
[31] Faisal F H M and Kamiński J Z 1998 *Phys. Rev. A* **58**, R19